Metab Brain Dis (2017) 32:1147–1161
DOI 10.1007/s11011-017-0012-6

ORIGINAL ARTICLE

Multidirectional inhibition of cortico-hippocampal neurodegeneration by kolaviron treatment in rats

Olayemi Joseph Olajide[1] · **Nnaemeka Tobechukwu Asogwa**[2,3] · **Blessing Oluwapelumi Moses**[1] · **Christiana Bidemi Oyegbola**[1]

Received: 20 October 2016 / Accepted: 6 April 2017 / Published online: 13 April 2017

Abstract Earliest signs of neurodegenerative cascades in the course of Alzheimer's disease (AD) are seen within the prefrontal cortex (PFC) and hippocampus, with pathological evidences in both cortical structures correlating with manifestation of behavioural and cognitive deficits. Despite the enormous problems associated with AD's clinical manifestations in sufferers, therapeutic advances for the disorder are still very limited. Therefore, this study examined cortico-hippocampal microstructures in models of AD, and evaluated the possible beneficial roles of kolaviron (Kv)-a biflavonoid complex in rats. Nine groups of rats were orally exposed to sodium azide (NaN_3) or aluminium chloride ($AlCl_3$) solely or in different combinations with Kv. Sequel to sacrifice and transcardial perfusion (using buffered saline then 4% paraformaldehyde), PFC and hippocampal tissues were harvested and processed for: spectrophotometric assays of oxidative stress and neuronal bioenergetics parameters, histological demonstration of cytoarchitecture and immunohistochemical evaluation of astrocytes and neuronal cytoskeleton. Results showed alterations in mitochondrial functions, which led to compromised neuronal antioxidant system, dysfunctional neural bioenergetics, hypertrophic astrogliosis, cytoskeletal dysregulation and neuronal death within the PFC and hippocampus. These degenerative events were associated with NaN_3 and $AlCl_3$ toxicity in rats. Furthermore, Kv inhibited cortico-hippocampal degeneration through multiple mechanisms that primarily involved halting of biochemical cascades that activate proteases which destroy molecules expedient for cell survival, and others that mediate a program of cell suicide in neuronal apoptosis. In conclusion, Kv showed important neuroprotective roles within cortico-hippocampal cells through multiple mechanisms, and particularly has prominent prophylactic activity than regenerative potentials.

Keywords Alzheimer's disease · Astrogliosis · Cytoskeleton · Neural bioenergetics · Oxidative stress

Introduction

Neuropathological alterations within the prefrontal cortex (PFC) and hippocampus are mostly involved in the progressive cognitive decline associated with AD clinical manifestation (Reitz and Mayeux 2014; Serrano-Pozo et al. 2011). Connections between the two cerebral structures are of primary behavioural relevance, as they play a major roles in the representation and enactment of memory, cognitive and emotional behaviour (Barbas 2009). The multifactorial etiopathogenic mechanisms involved in AD (and other neurodegenerative disorders) has limited understanding of the loss of molecular substrates necessary for normal cortico-hippocampal connectivity and function during progression of the disease; thereby leading to difficulties in the evolution of potent molecules necessary for therapy. Though unsatisfactory, characterisation of the mechanisms involved in neuronal death at the cellular and molecular levels, has led to the proposition of various therapeutic strategies. In the context of AD, it is speculated that treatments that interferes with the pathogenic mechanisms would be able to

✉ Olayemi Joseph Olajide
olajide.oj@unilorin.edu.ng; olajide.olayemijoseph@gmail.com

[1] Division of Neurobiology, Department of Anatomy, Faculty of Basic Medical Sciences, University of Ilorin, Ilorin, Nigeria

[2] Department of Biochemistry, Faculty of Life Sciences, University of Ilorin, Ilorin, Nigeria

[3] Central Research Laboratories Ltd, 132b University Road, Ilorin, Nigeria

slow down or ultimately stop the evolvement of the diseases (Merelli et al. 2013).

In like manner, kolaviron (Kv) – a biflavonoid isolate of seeds of *Garcinia kola* (Gk), is known to have some biological advantages in certain diseases. Gk plant is highly valued and essential in African folklore medicine owing to its varied social and medicinal uses. Many useful phytochemicals have been isolated from Gk seeds, but Kv is by far the most important, with a well-defined structure (Farombi and Owoeye 2011) as shown in Fig. 1. The ability of Kv to both slow down and prevent the rate of tissue damage has been described in vivo and in vitro (Farombi et al. 2013; Oyenihi et al. 2015). Free radicals and other reactive oxygen species (ROS) are generated continuously via normal physiological processes and more so in pathological conditions. Compounds such as sodium azide (NaN_3) and Aluminium chloride ($AlCl_3$) are known to compromise neuronal mitochondrial oxidative complexes, thereby increasing the production of ROS (Rodella et al. 2008; Wood et al. 2012). When in enormous proportion, ROS reacts with nitrogen molecules within cells and form nitric oxide (NO) and reactive nitrogen species (RNS). Proteins involved in these pathways are often mutated as a result of cellular toxicity from the free radicals (Trushina and McMurray 2007), initiating DNA cleavage and neuronal death-as seen in AD (Lanni et al. 2012; Patten et al. 2010). Precisely, subcellular alterations similar to those seen in AD, have been described in the neurotoxic mechanisms involved in each of NaN_3 and $AlCl_3$-induced neurodegeneration (Reitz et al. 2011; Szabados et al. 2004). Furthermore, $AlCl_3$ and NaN_3 are suitable models of neurodegenerative conditions in mammals as there is progression of disease development in a properly positioned manner, wherein behavioural deficits result from changes in normal molecular and metabolic equilibrium, followed by histopathological disruptions, thereby mimicking the cascades of events in AD, which is necessary for pharmacotherapeutic applications (Jellinger 2010; Wood et al. 2012). Building on this background, our study sought to investigate the probable inhibitory mechanisms of Kv on molecular, metabolic and cellular disruptions in two drug models of AD.

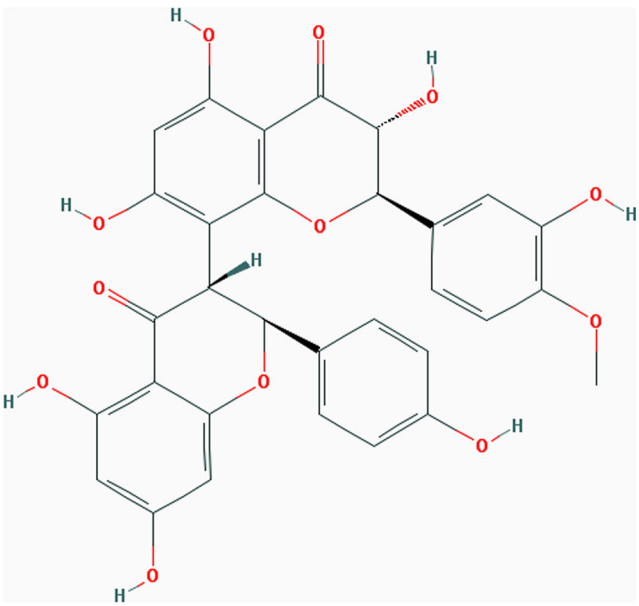

Fig. 1 Chemical structure of kolaviron consisting of Garcinia biflavonoid-1 (GB_1), Garcinia biflavonoid-2 (GB_2) and Kolaflavanone in the ratio 2:2:1

Materials and methods

Materials

$AlCl_3$, NaN_3, 3′3′-Diaminobenzidine tetrachloride and methenamine silver intensification kits salts were procured from Sigma-Aldrich (Germany). Phosphate buffered saline (PBS; pH 8.0) was freshly prepared. Superoxide Dismutase (SOD), Glutathione Peroxidase (GPx), Glucose-6-phosphate dehydrogenase (G6PDH) and Lactate dehydrogenase (LDH) assay kits were acquired from Abcam®, USA. Rat anti-GFAP and anti-NF were purchased from Cell Signalling Technologies, Massachusetts, USA. Fifty-four (54) male Wistar rats (9 weeks old) were housed at the animal holding facilities of the Faculty of Basic Medical Sciences, University of Ilorin, Nigeria, where they had liberal access to rat chow and water. Ethical clearance was sought and obtained from the College of Health Sciences Ethical Committee, University of Ilorin, Nigeria. Animal handling and protocols were also carried out in strict compliance to the National Institutes of Health guide for the care and use of Laboratory animals (NIH Publications No. 8023, revised 1978). *Garcinia kola* (seeds) was sourced from a market in Ilorin, Nigeria and verified to match specimen 'UILH/001/1217' at the herbarium of Botany Department, Faculty of Life Sciences, University of Ilorin.

Extraction and identification of kolaviron

Isolation of Kv from dry seeds of *Garcinia kola* and characterisation was done with some modifications to the method published by Farombi et al. (2009). Summarily, seeds were pulverized into fine powder using an electric blender. Extraction from the powdered seeds was then carried out with light petroleum ether (boiling point (b.p.) 40–60 °C) in a soxhlet extractor placed in an electric water bath for 24 h. Thereafter, the defatted, dried marc was repacked and extracted with acetone (b.p. 56–60 °C) in the water bath for 14 h. The resultant extract was then concentrated and diluted twice its volume with distilled water and then extracted with ethyl acetate (7.250 ml). The concentrated ethyl acetate fraction gave a yellow solid (Kv). Identity of Kv was determined by subjecting the concentrate to thin layer chromatograph using

Silica gel GF 254-coated plates and solvent mixture of methanol and chloroform in a ratio of 1:4 *v*/v. The separation revealed the presence of three bands which were viewed under UV light at a wavelength of 254 nm with RF values of 0.48, 0.71 and 0.76. The yield of Kv preparation in this study was 7.3%. Kv was kept at a temperature of 4 °C before and after each use.

Preparation of solutions

Kv was dissolved in corn oil (Carlini, ALDI Inc. Batavia) (80 mg/ml) which served as vehicle for oral treatment. Both NaN_3 and $AlCl_3$ salts were dissolved in distilled water (20 mg/ml) and adjusted to pH 7.4 with 0.1 M phosphate-buffered saline (PBS). All solutions were prepared newly on each morning of administration and kept at 4 °C before use. A modified orogastric cannula was used to administer treatment solutions to rats.

Animal grouping and treatment regimen

Using random assortment method, rats were grouped into nine (9) labelled A - I (n = 6). A received PBS (2 ml) daily for 28 days; B received 2 ml of corn oil (CO) daily for 14 days; C received 200 mg/kgBw Kv daily for 14 days; D received 15 mg/kgBw NaN_3 daily for 14 days; E received 100 mg/kgBw $AlCl_3$ daily for 14 days; F received simultaneous 15 mg/kgBw NaN_3 and 200 mg/kgBw Kv daily for 14 days; G received simultaneous 100 mg/kgBw $AlCl_3$ and 200 mg/kgBw Kv daily for 14 days; H received 15 mg/kgBw NaN_3 daily for 14 days followed by 200 mg/kgBw Kv for the subsequent 14 days; and I received 100 mg/kgBw $AlCl_3$ daily for 14 days followed by 200 mg/kgBw Kv for the subsequent 14 days.

Sacrifice, brain sample collection and tissue processing

Sequel to last the administration, intraperitoneal injection of 20 mg/KgBw ketamine was used to euthanize rats for histology and immunohistochemistry. Rats were then perfused transcardially, first with a flush of 50 ml 0.1 M PBS (pH 7.4) and then with 500 ml of 4% paraformaldehyde (PFA). Excised brains were then rinsed in 0.25 M sucrose 3 times for 5 min each and then post fixed in 4% PFA for 24 h before being stored in 30% sucrose at 4 °C until further processing. Rats for enzymatic assays were sacrificed by quickly separating the head from the trunk, to avoid the interference of ketamine with biochemical redox; brains were then excised, rinsed in 0.25 M sucrose 3 times for 5 min each and placed in 30% sucrose in which they were stored at 4 °C. Coronal sections of PFC and hippocampus were obtained stereotaxically (+4 mm and −3 mm from the bregma respectively) from each brain. Subsequently, sections were processed routinely to obtain paraffin wax embedded blocks for histology and antigen retrieval immunohistochemistry. Histological staining was carried out in paraffin wax embedded sections which were stained in Haematoxylin and Eosin using the methods described by Fischer et al. (2005).

Immunohistochemistry

Prefrontal and hippocampal serial sections (15 μm) were taken from paraffin blocks to glass slides and protein cross-linkages were removed by applying 0.1% trypsin for 20 min at room temperature to activate the antigens. Hydrogen peroxide was used to block endogenous peroxidase, while 5% bovine serum albumin (BSA) was used to reduce non-specific protein reactions. Diluted primary antibody was added to each slide (500 ml) and incubated overnight at 4 °C. Primary antibodies (anti-GFAP and anti-NF) dilution was done in blocking buffer (10% calf serum with 1% BSA and 0.1% Triton X-100 in 0.1 M PBS): with both diluted at 1:100. Following this, secondary biotinylated antibody were desalted and diluted in PBS (pH 7.4) prior to its application on tissue sections. Incubation with secondary antibody was done in the humidity chamber for 30 min at room temperature. Immunogenic reaction was developed using 3′3′ Diaminobenzidine tetrachloride (DAB) and intensified using methenamine silver kit. Both PFC and hippocampal sections were counterstained in haematoxylin, and subsequently treated in 1% acid alcohol to reduce the counterstain intensity. Histology and IHC images were acquired using an Olympus binocular research microscope (Olympus, New Jersey, USA) connected to an Amscope Camera (5.0 MP).

Spectrophotometry for enzymatic assays

Determination of SOD, GPx, G-6-PDH and LDH activities was carried out in PFC and hippocampal tissues of the rats using spectrophotometric technique. Each of the assay kits were procured from Cell Signalling Technologies, Danvers, USA. Dissected brains (in sucrose at 4^0 C) from rats across groups were weighed and pulverized in 0.25 M sucrose (Sigma) with the aid of an automated homogenizer at 4 °C. Lysates from PFC and hippocampus were centrifuged for 10 min in a microfuge at 12,000 rpm to obtain the supernatant containing organelle fragments and synaptosomes. The supernatants were aspirated into plain labelled glass cuvette placed in ice. SOD, GPx, G-6-PDH and LDH activities were assayed according to manufacturer's instruction in each assay kit pack.

Quantitative data analysis

Results obtained from quantitative studies were analysed using GraphPad Prism® software (Version 6.1). SOD, GPx, G-6-PDH and LDH values in prefrontal and hippocampal

lysates across treatment groups were evaluated by analysis of variance (ANOVA) with Tukey's multiple comparisons test. Significance was set at $p < 0.05$. Bar charts were used to represent outcomes with error bars showing the mean ± standard error of mean respectively.

Results

Kolaviron improves antioxidant defense system and inhibits cortico-hippocampal oxidative toxicity

Differential expression of major antioxidant enzymes were assessed in this study, to investigate their involvement in the degenerative processes associated with NaN_3 and $AlCl_3$-induced toxicity and to understand mechanisms involved in Kv's inhibitory roles. Results from spectrophotometric assay of SOD profiles from PFC and hippocampal lysates showed close similarities in patterns of expression (Fig. 2a, b). In the PFC, control rats that received PBS (A), CO (B) and Kv (C) expressed normal SOD levels with slight increase seen in group C compared to the other two groups. The antioxidant profile in rats treated with either of NaN_3 (D) or $AlCl_3$ (E) were however depleted within the PFC as level of SOD significantly reduced compared to the control. Kv showed little restorative potentials in improving the antioxidant status of rats that received it after either of NaN_3 (F) or $AlCl_3$ (G)-induced oxidative dysfunction, as SOD profiles in both groups are indifferent statistically from neither the control nor the neurotoxicity groups (D and E). Neuroprotective role of Kv was evident in PFC of rats in which it was treated simultaneously with either of NaN_3 (H) or $AlCl_3$ (I). Although in both groups, PFC SOD profiles were upregulated to levels quite similar to the control, the differences were not significantly different from groups D and E. Furthermore, expressed SOD in hippocampal lysates of control rats, which received PBS (A), CO (B) and Kv (C) were at similar levels. On the hand, rats treated with NaN_3 (D), NaN_3 then Kv (F) and $AlCl_3$ then Kv (F) show considerable increased SOD profiles compared to the control groups. However, these changes are not significant statistically. Additionally, rats treated $AlCl_3$ (E) shows significant increase in hippocampal levels of SOD when compared with the controls (A, B and C). Hippocampal SOD expressions in rats that received Kv simultaneously with either NaN_3 (H) or $AlCl_3$ (I) are closely similar to the levels in the control, with H being significantly lesser than levels in group E, while I is not significantly different from other treatment groups. Another antioxidant enzyme examined within prefrontal and hippocampal lysates in this study was GPx. Results in Fig. 3a shows that control rats, which received PBS (A), CO (B) and Kv (C) expressed higher GPx levels, compared to rats that were treated either of NaN_3 (D), $AlCl_3$ (E), NaN_3 then Kv (F) or $AlCl_3$ then Kv (G). Furthermore, expressed prefrontal GPx levels in groups D, F and G are significantly lower than in the control groups, reflecting depletion in the antioxidant defense system within cortical cells.

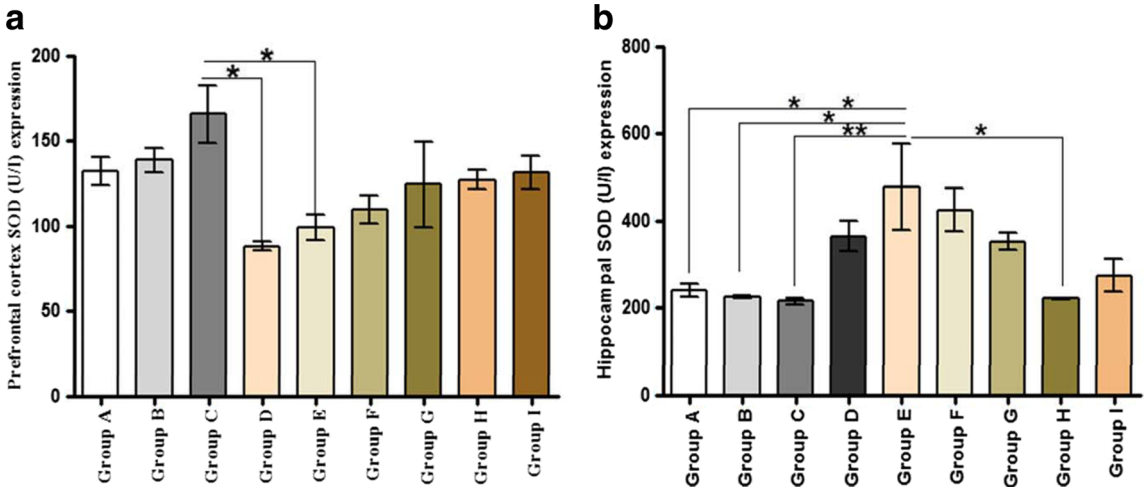

Fig. 2 **a** PFC SOD expressed in lysates from rats across treatment groups. Groups that received PBS (A), CO (B) and Kv (C) have similar SOD activities. However, administration of both NaN_3 (D) and $AlCl_3$ (E) depleted prefrontal SOD activities in comparison with group C. Kv treatment improved SOD profiles within PFC following NaN_3 (F) or $AlCl_3$ (G)-induced neurotoxicity-as levels are similar to control but insignificant from D and E. Rats treated Kv simultaneously with either NaN_3 (H) or $AlCl_3$ (I) shows up-regulated PFC SOD profiles which are closely similar to the control. **b** Hippocampal SOD activities expressed in lysates from treated rats. Control rats which received PBS (A), CO (B) and Kv (C) have similar hippocampal SOD expression while rats treated with NaN_3 (D), NaN_3 then Kv (F) and $AlCl_3$ then Kv (H) have considerable increased SOD profiles compared to the control. Additionally, rats treated $AlCl_3$ (E) shows significant increase in hippocampal levels of SOD when compared with the control (A, B and C). Hippocampal SOD expressions in rats that received Kv simultaneously with either NaN_3 (H) or $AlCl_3$ (I) are closely similar to the levels in the control, with H significantly lesser than in group E, while I is not significantly different from other treatment groups. Values are expressed as the mean ± SE ($n = 4$ per group and * = $p < 0.05$; ** = $p < 0.01$)

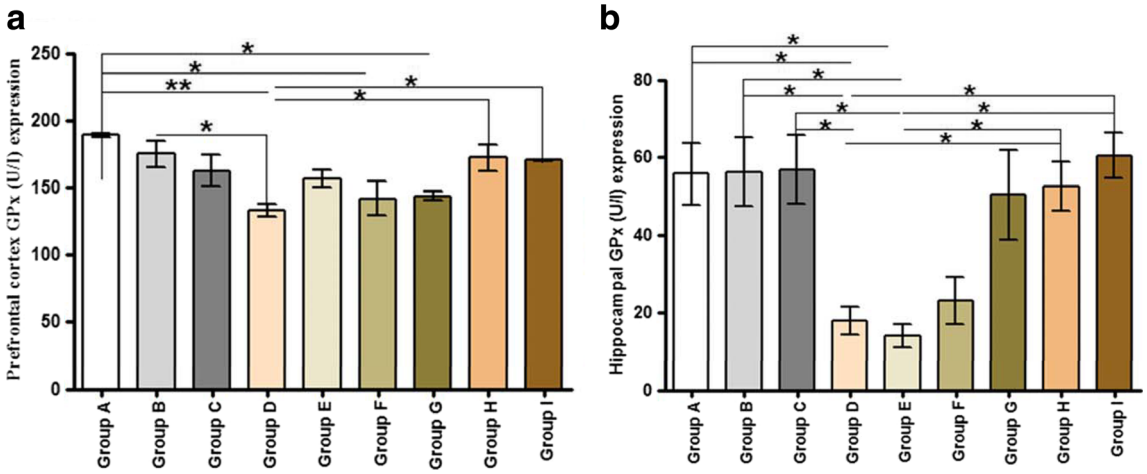

Fig. 3 **a** GPx expression in PFC lysates from treated rats. Rats that received PBS (A), CO (B) and Kv (C) and served as controls expressed higher GPx levels, compared to rats that received NaN_3 (D), $AlCl_3$ (E), NaN_3 then Kv (F) and $AlCl_3$ then Kv (G). Expressed GPx levels in groups D, F and G are significantly lower than in the control groups (precisely A and B). Kv treatment significantly restored GPx expression to the control levels in PFC of rats that received it simultaneously with either NaN_3 (H) or $AlCl_3$ (I). This is further shown by the significant upregulation of GPx in both groups (H and I) compared to the level expressed in group D. **b** Hippocampal GPx levels expressed in lysates across treatment groups. PBS (A), CO (B) and Kv (C) treated rats have similar hippocampal GPx activities. Conversely, Gpx expression was enormously reduced in rats treated NaN_3 (D), $AlCl_3$ (E) and NaN_3 then Kv (F) compared to the control groups, with D and E showing statistical significance. Again, hippocampal GPx levels were significantly upregulated in groups administered Kv simultaneously with either of NaN_3 (H) or $AlCl_3$ (I). Expressed GPx in H and I are similar to the control groups, and are also significantly higher than the levels in groups D and E; underpinning Kv roles in preventing oxidative neurotoxicity. Values are expressed as the mean ± SE ($n = 4$ per group and * = $p < 0.05$; ** = $p < 0.01$)

Again, the protective potentials of Kv were demonstrated significantly within the PFC of rats that received the complex simultaneously with either NaN_3 (H) or $AlCl_3$ (I), as GPx expression in both groups is in similarity with the control levels. This is further shown by the significant upregulation of GPx in both groups (H and I) compared to the level expressed in group D. Similarly, hippocampal lysates GPx expression shown in Fig. 3b, revealed that PBS (A), CO (B) and Kv (C) treated rats have very similar levels of the enzymes within neural cells. Conversely, Gpx expression was enormously reduced in rats treated NaN_3 (D), $AlCl_3$ (E) and NaN_3 then Kv (F) compared to the control groups, with groups D and E particularly significantly lower. Again, hippocampal GPx levels were normalised/upregulated in rats administered Kv simultaneously with either of NaN_3 (H) or $AlCl_3$ (I). Not only were the expressed GPx levels in groups H and I similar to the control groups, they are significantly higher than the levels in groups D and E, underpinning Kv roles in preventing oxidative toxicity.

Modulation of cortico-hippocampal bioenergetics dysfunctions by kolaviron

Glucose metabolizing enzymes which are important in neural energy production were assessed in our experiment, to study shifts in metabolic machinery within prefrontal and hippocampal cells from NaN_3 or $AlCl_3$-induced neurotoxicity while investigating mechanisms of Kv's inhibitory roles respectively. Assessment of prefrontal LDH levels shown in Fig. 4a, reveals that rats treated PBS (A), CO (B) and Kv (C) have similar levels of expressed LDH within lysates. In contrast, cortical LDH was significantly upregulated in rats treated with NaN_3 (D) and $AlCl_3$ (E) when compared with its expressions in the control groups, suggesting a shift to stress-related energy metabolism within neurons. Intriguingly, Kv treatment significantly normalized the expression of LDH within the PFC of rats that received it concomitantly with either of NaN_3 (H) or $AlCl_3$ (I). Both groups expressed very similar LDH levels with the control rats and are much different from LDH levels in groups D and E. In addition, impaired cortical bioenergetics induced by NaN_3 and $AlCl_3$ treatment was improved to levels similar with the control levels by Kv, as seen by expressed LDH in groups F and G respectively. However, it is noteworthy that the differences in LDH expression between groups F and G and D and E are not significant, unlike in H and I. Regarding hippocampal LDH expressions, results from study (Fig. 4b) showed similarity to the expression of LDH within the PFC. Rats in the control groups, treated PBS (A), CO (B) and Kv (C) have close levels of LDH expression within hippocampal homogenate. In line with previous results of this study, NaN_3 and $AlCl_3$ treatments (groups D and E) significantly dysregulated hippocampal bioenergetics and shifted it to the stress-related state by upregulating LDH levels in comparison with the control. Additionally, hippocampal LDH levels are restored significantly to normal in rats that received Kv alongside either of NaN_3 (H) or $AlCl_3$ (I) treatment, in comparison with groups D and E. Although, Kv treatment in rats that were pre-administered NaN_3 (F) or $AlCl_3$ (G) have

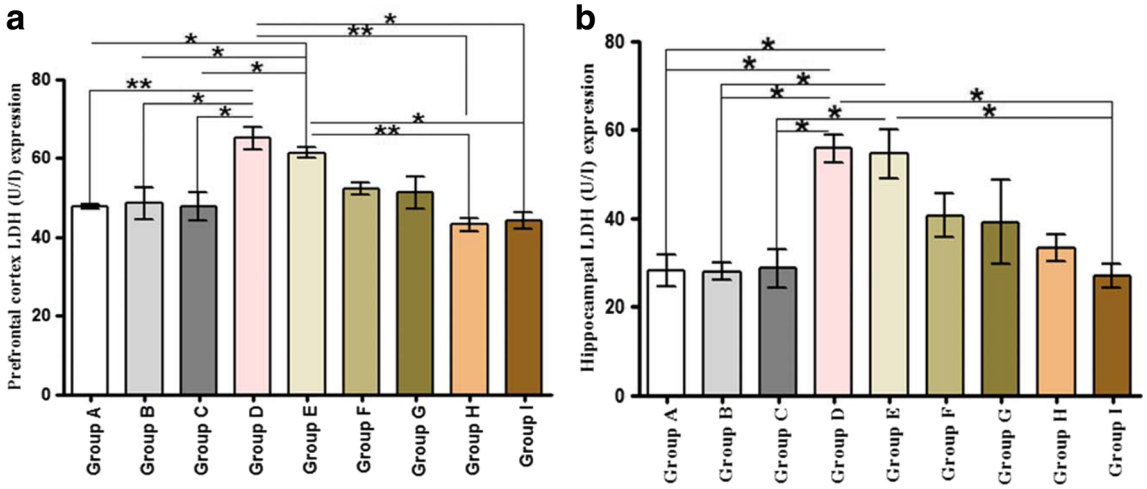

Fig. 4 **a** Expressed LDH in PFC lysates across treatment groups. Rats treated PBS (A), CO (B) and Kv (C) shows similar levels of LDH within cortical homogenate. Contrastingly, LDH was significantly upregulated in rats treated with NaN_3 (D) and $AlCl_3$ (E) when compared with control. Kv significantly normalized the expression of LDH within the PFC of rats that received it concomitantly with either of NaN_3 (H) or $AlCl_3$ (I) compared to D and E. **b** Hippocampal LDH levels expressed in lysates across treatment groups. Rats that served as control and received PBS (A), CO (B) and Kv (C) shows closely similar LDH expression within hippocampal homogenates. Again, NaN_3 and $AlCl_3$ treatments (D and E) significantly dysregulated hippocampal bioenergetics and shifted it to the stress-related state by upregulating LDH levels in comparison with the control. Hippocampal LDH levels were significantly restored to normal in rats that received Kv alongside either of NaN_3 (H) or $AlCl_3$ (I) treatment (compared to D and E). Although, Kv treatment lowered LDH expression in rats that were pre-administered NaN_3 (F) or $AlCl_3$ (G), the differences are insignificant when compared to groups D and E. Values are expressed as the mean ± SE ($n = 4$ per group and * = $p < 0.05$; ** = $p < 0.01$)

lowered LDH expression within hippocampal cells, the differences are insignificant when compared to groups D and E. Neural activities of G6PDH were also assessed in prefrontal and hippocampal lysates in this study. Findings in Fig. 5a shows notable alterations in G6PDH activities within prefrontal homogenates of treated rats with unspecific expression patterns across groups. Control rats, which were treated with either of PBS (A), CO (B) or Kv (C), have almost similar levels of G6PDH, with group C showing slightly higher level. Furthermore, rats treated simultaneously with Kv and NaN_3 (H) shows the highest G6PDH activity, and is significantly more than levels expressed in control groups (A, B); and in rats that received Kv after either of NaN_3 (F) or $AlCl_3$ (G) treatments. Surprisingly, the expressed G6PDH in rats treated NaN_3 (D) or $AlCl_3$ (E) are not significantly different from other treatment groups. Figure 4b further shows hippocampal G6PDH levels expressed in lysates across treatment groups. Similar to the patterns of G6PDH expression within the PFC-which is seemingly erratic, hippocampal activities of the G6PDH is not significantly ($p < 0.05$) different across treatment groups in this study. However, rats treated with PBS (A), $AlCl_3$ (E), and NaN_3 with simultaneous Kv (H), shows the highest G6PDH activities, while the levels in rats treated CO (B), NaN_3 then Kv (F) and $AlCl_3$ simultaneously with Kv (H) are evidently the same. Group C rats which received Kv alone, have the least G6PDH level, while rats that received Kv simultaneously with $AlCl_3$ have a similarly low expression of the enzyme.

Inhibitory roles of kolaviron in prefrontal and hippocampal cytoarchitectural degeneration

Histological studies help reveal specific cell modes and mechanisms that results from physiological alterations and mediate behavioural changes in neurodegenerative conditions, providing good platform for seeking effective therapeutic interventions. Prefrontal and hippocampal histology were demonstrated with H and E staining methods in this study. Figure 6a shows morphological presentations of prefrontal cortex layers, which are distinctly demarcated by presence of different cell types and distribution. Rats treated either of PBS (A), CO (B) or Kv (C) shows regular neuronal population, normal cytoarchitecture and distinguished cortical layers of PFC with healthy neurons indicated by blue arrows. However, histological alterations are seen in neurons of rats treated NaN_3 (D) or $AlCl_3$ (E) across the neuropil. In both groups, pyramidal neurons in layers III and V are mostly degenerated, having cytoplasmic fragmentation and aggregation of nuclear material as shown by red arrows. Although degenerating neurons are observable within PFC of rats that received Kv therapy after NaN_3 (F) or $AlCl_3$ (G) treatment, there are some improvement in cell sub-population and morphology across the prefrontal layers compared to groups D and E. Notably, neuronal morphology within the neuropil of rats that received Kv with concomitant treatment of NaN_3 (H) or $AlCl_3$ (I) have very similar cortical cytoarchitecture with the control groups. Similarly, Fig. 6b shows general hippocampal sections of treated rats stained with H and E. Rats that received PBS

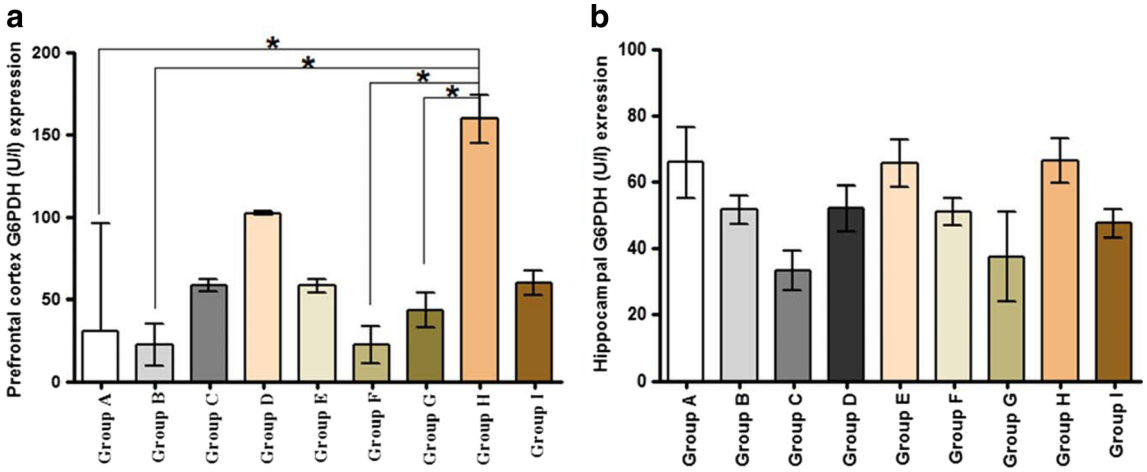

Fig. 5 **a** Expression of G6PDH in PFC lysates across treatment groups. Alterations in G6PDH activities within prefrontal homogenates in treated rats are in no specific patterns. Control rats treated either of PBS (A), CO (B) or Kv (C) has similar G6PDH activities, with group C showing a slight deviation. Furthermore, rats treated simultaneously with Kv and NaN_3 (H) shows the highest G6PDH activity, and is significantly higher than in control groups (A, B) and in rats that received Kv after either of NaN_3 (F) or $AlCl_3$ (G). Expressed G6PDH in rats treated NaN_3 (D) or $AlCl_3$ (E) are not significantly different from other treatment groups. **b** Expressed G6PDH in hippocampal lysates from the different treatment groups. Activities of G6PDH in hippocampus of treated rats are also not significantly different. However, rats treated PBS (A), $AlCl_3$ (E), and NaN_3 with simultaneous Kv (H), showed the highest G6PDH activities, while the levels in rats treated CO (B), NaN_3 then Kv (F) and $AlCl_3$ simultaneously with Kv (H) are observably the same. Rats treated Kv shows the least G6PDH activities, while rats that received Kv simultaneously with $AlCl_3$ have a similarly low expression of the enzyme. Values are expressed as the mean ± SE ($n = 4$ per group and * = $p < 0.05$)

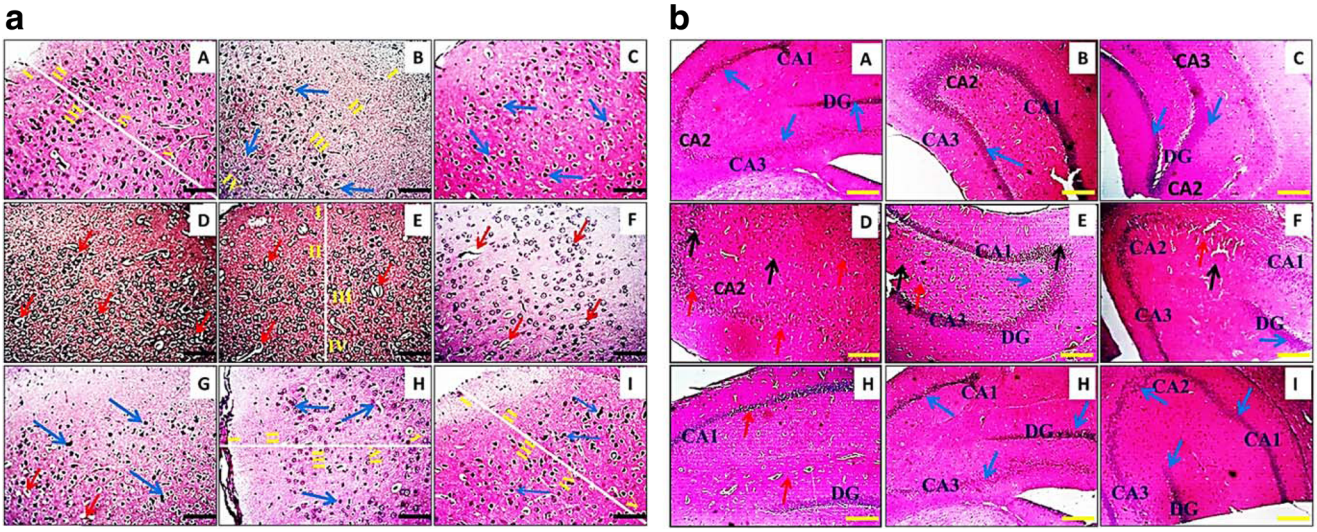

Fig. 6 **a** General histology of PFC from treated rats stained in H and E with morphological layers (I - IV) demarcated by cell types and distribution. Rats treated PBS (A), CO (B) and Kv (C) shows regular neuronal population, normal cytoarchitecture and distinguished prefrontal layers-with regular neurons (*blue arrows*). Neurons with degenerative features scatters within neuropil of rats treated NaN_3 (D) or $AlCl_3$ (E). In both groups, pyramidal neurons in layers III and V are mostly degenerated, and are characterised by cytoplasmic fragmentation and aggregation of nuclear materials (*red arrows*). Few degenerating neurons are observable within PFC of rats that received Kv therapy after NaN_3 (F) or $AlCl_3$ (G) treatment, but there are cytological improvement in cell sub-population and general morphology compared to D and E. Prefrontal neuronal morphology of H and I groups have close similarities with the control groups. **b** Panoramic view of hippocampal general morphology of treated rats shown in H and E. Rats that received PBS (A), CO (B) or Kv (C) shows normal hippocampal morphology as cells in these control rats are in normal arrays (*blue arrows*) and characterized by distinct arrangement of pyramidal neurons within the cornu ammonis (CA1-CA3) to the granule cells of the dentate gyrus (DG). Hippocampal section from NaN_3 (D) and $AlCl_3$ (E)-treated rats shows several pyknotic changes, with disorderly pyramidal/granular neurons (red arrows) observable within the severely fragmented framework (*black arrows*). Groups treated Kv after either of NaN_3 (F) or $AlCl_3$ (G) shows slight degenerative characteristics (*black and red arrows*), with little improvement over D and E. However, hippocampal morphological alteration and cellular degeneration was profoundly halted by Kv in rats that received it simultaneously with either of NaN_3 (H) or $AlCl_3$ (I). CA and DG in both groups are similar to the control in terms of cellular arrangement, disposition and expression. (Scale bars: 400 μm)

(A), CO (B) or Kv (C) (control groups) shows normal hippocampal morphology from the demonstrated panoramic sections. Hippocampal cells in these groups are in normal arrays (blue arrows), as observed in the distinct arrangement of pyramidal neurons within the cornu ammonis (CA 1–3) to the granule cells of the dentate gyrus (DG). Again, hippocampal neuronal degeneration was induced by the administration of NaN_3 (D) and $AlCl_3$ (E). Several pyknotic and disorderly pyramidal/granular neurons (red arrows) can be seen within the fragmented/disjointed neuropil and cytoskeletal framework (black arrows). Furthermore, induced degenerative changes in the hippocampus was characterised by fragmented pyramidal and granule cell layer, particularly in group D. Also, hippocampal histology in groups treated Kv after either of NaN_3 (F) or $AlCl_3$ (G) shows slight degenerative characteristics (black and red arrows), similar to groups D and E. Cellular disposition within CA and DG of both groups are however better structured and delineated (blue arrows). Hippocampal cells morphological alteration was halted profoundly in rats in which it was given simultaneously with either of NaN_3 (H) or $AlCl_3$ (I). CA and DG in both groups showed similar cellular dispensation as seen in the control groups.

Cortico-hippocampal neuronal morphology was further demonstrated at higher power magnification, to show changes resulting from treatments in this study. Figure 7a shows that morphology of neurons in the pyramidal cell layer of PFC consist of normal cell bodies and cell processes within cortical sections of control rats, which were treated PBS (A), CO (B) and Kv (C). Cytoplasmic organelles, nuclear materials and neuronal membrane are greatly compromised within cortical sections of rats treated NaN_3 (D), $AlCl_3$ (E) and in rats that received Kv after NaN_3 (F) treatment. In addition, vacuoles surround cell membranes of the degenerating pyramidal neurons in groups D and E and a few of the neurons in group F. However, the morphology of pyramidal neurons within PFC of rats treated with Kv after $AlCl_3$ (G) shows some improvement over those in groups D, E and F but with a few pyknotic pyramidal cells. On the other hand, PFC of rats treated with Kv concomitantly with either of NaN_3 (H) or $AlCl_3$ (I) have neurons with preserved processes and cell bodies within the neuropil as seen in the control groups. Additionally, Fig. 7b shows that neuronal morphology in hippocampal sections, particularly pyramidal neurons and neuroglia within CA1-CA2 of control rats-treated with PBS (A), CO (B) are Kv (C) have normal cell bodies with dendritic and axonal

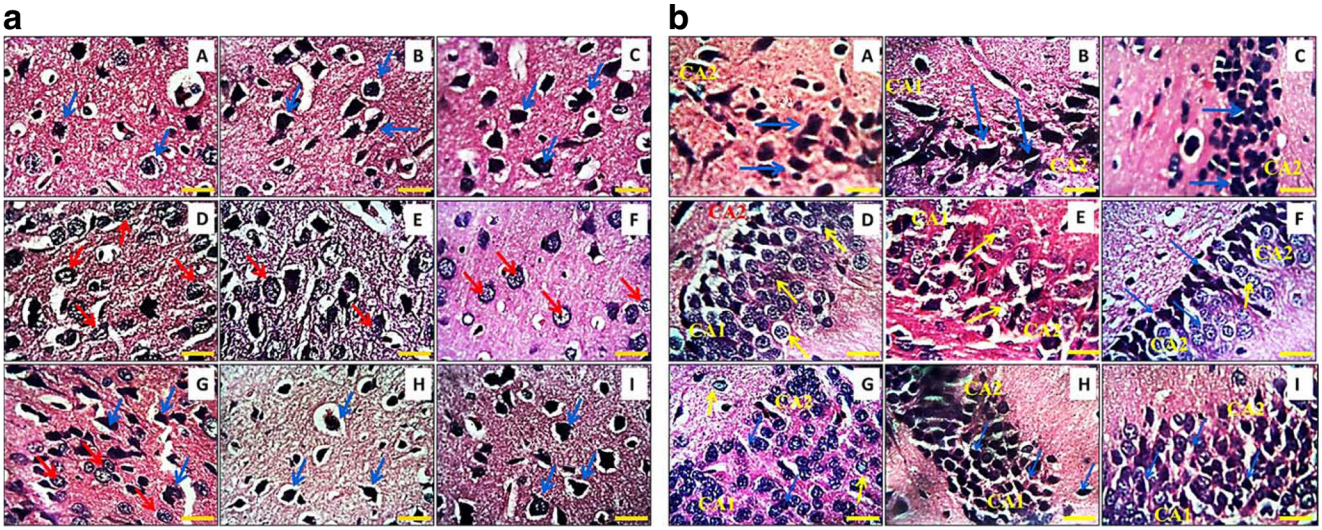

Fig. 7 **a** Neuronal morphology in the pyramidal cell layers of PFC shown by H and E staining. Pyramidal neurons with normal cell bodies and cell processes (*blue arrows*) are seen within prefrontal sections of rats treated PBS (A), CO (B) and Kv (C). Cytoplasmic inclusions, nuclear materials and neuronal membrane are greatly compromised (*red arrows*) within prefrontal sections of rats that received NaN_3 (D), $AlCl_3$ (E), and in Kv after NaN_3 (F) treated rats. Vacuoles are observable surrounds cell membranes of the degenerating pyramidal neurons in groups D and E and few in F. PFC pyramidal neurons in rats treated with Kv after $AlCl_3$ (G) shows morphological improvement over those in groups D, E and F, but a few pyknotic pyramidal cells are present. PFC sections of rats treated with Kv concomitantly with either of NaN_3 (H) or $AlCl_3$ (I) are characterized by neurons with preserved processes and cell bodies and are similar to controls. **b** Cells in hippocampal sections of treated rats shown by H and E staining. Pyramidal neurons and neuroglia within CA1-CA2 of control rats which received PBS (A), CO (B) or Kv (C) have normal cell bodies with dendritic and axonal processes that are well expressed across hippocampal neuropil (*blue arrows*). Degenerative changes in hippocampal pyramidal neurons and neuroglia within CA1-CA2 in NaN_3 (D) and $AlCl_3$ (E) treated rats are hallmarked by pyramidal neurons with clustered cell bodies, extruded cytoplasmic contents, indistinct nuclear demarcation, short projections and fusion of adjacent neuronal membranes (*red arrows*). Rats administered Kv after treatment with either NaN_3 (F) or $AlCl_3$ (G) shows improved neural morphology within hippocampal (CA1-CA2) sections (*blue arrows*), although a few degenerative features are shown in F, which has neurons with condensed nuclei (*red arrows*). Kv prevented degeneration of hippocampal pyramidal neurons in rats that received it simultaneously with either of NaN_3 (H) or $AlCl_3$ (I). Neurons in both groups are succinctly expressed with a well-delineated cytoarchitecture which is similar to control. (Scale bars: 25 μm)

processes that are clearly demonstrated within the neuropil. In similarity with neuronal toxicity seen in the PFC, degenerative changes to hippocampal pyramidal neurons and neuroglia within CA1-CA2 also resulted from NaN_3 (D) and $AlCl_3$ (E) treatment. Cell bodies of pyramidal neurons in both groups are clustered, showing extruded contents, indistinct nuclear demarcation, short projections and fusion of adjacent neuronal membranes. Rats administered Kv after treatments with either NaN3 (F) or AlCl3 (G) have improved neuronal morphology within hippocampal (CA1-CA2) sections (blue arrows) although a few degenerative features can be seen, particularly in group F (red arrows). The neuroprotective mechanism of Kv was further shown within hippocampal cells, as it prevented pyramidal cells degeneration in rats that received it simultaneously with either of NaN_3 (H) or $AlCl_3$ (I). Cellular morphology is well delineated/outlined and similar to those in the control groups in these groups.

Kolaviron inhibits cortico-hippocampal cytoskeletal dysregulation and astrogliosis

Astrocytes and neurofilaments were demonstrated through immunohistochemical labelling (GFAP and NF-l respectively), to study their morphology and distribution within cortical and hippocampal sections of treated rats. Figure 8a shows that GFAP immunoposistive cells within PFC sections of rats that received PBS (A), CO (B) and Kv (C) are normal, sparsely and evenly expressed within the cortex; with evidences of almost identical morphological pattern seen within the three groups. Stained astrocytes appear hypertrophied and clustered within the PFC of rats treated with NaN_3 (D) and $AlCl_3$ (E), particularly within the external pyramidal cell layers, depicting initiation of astrogliosis by the neurotoxic molecules within the PFC. On the other hand, deposition of astrocytes within PFC of rats administered Kv after either of NaN_3 (F) or $AlCl_3$ (G) treatments are quite reduced, compared to groups D and E, but more than those expressed in the PFC of control rats. It was obvious that levels and patterns of astrocyte expression within PFC of rats treated with Kv simultaneously with either of NaN_3 (H) or $AlCl_3$ (I) are not different from the controls. In addition, Fig. 8b shows hippocampal astrocytes morphology and distribution in treated rats. Again, hippocampal sections of rats which served as control and received PBS (A), CO (B) and Kv (C) expressed few, normal astrocytes with numerous processes that are evenly distributed between neurons. It is noteworthy, that the general hippocampal morphology in the control groups is distinctly demonstrated, in concordance with general histological observations seen in

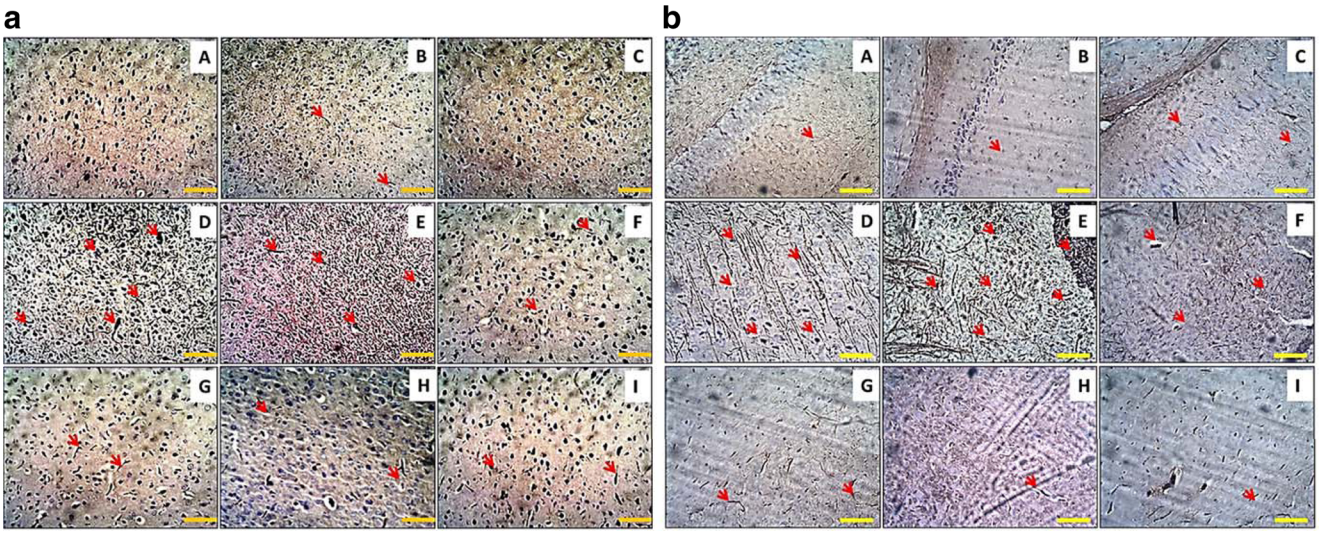

Fig. 8 **a** Immunohistochemical labelling of astrocytes (GFAP) in PFC sections of treated rats. Immunopositive cells within prefrontal sections of rats that received PBS (A), CO (B) and Kv (C) are sparsely and evenly expressed within the cortex, and shows identical morphological patterns. Hypertrophied astrocytes with modified processes appear in clusters within PFC of rats treated with NaN_3 (D) and $AlCl_3$ (E) (*red arrows*), particularly within the external pyramidal cell layer. Expression of astrocytes within PFC of rats administered with Kv after either of NaN_3 (F) or $AlCl_3$ (G) treatments are quite normal, compared to groups D and E with slight differences from the control. Evidently, mode and pattern of expressed astrocytes within prefrontal sections of rats treated Kv simultaneously with either of NaN_3 (H) or $AlCl_3$ (I) are normal and not different from controls. **b** Immunohistochemical labelling of astrocytes (GFAP) in hippocampal sections of treated rats. Thin sections from control rats that received PBS (A), CO (B) and Kv (C) expressed astrocytes with numerous astrocytic processes-that are evenly distributed around neurons (*arrows*). Rats treated with either of NaN_3 (D) or $AlCl_3$ (E) shows increased astroglia deposition and hypertrophy across hippocampal sections. Also, both groups show morphological irregularities with hippocampal regions are hardly appreciable. Expressed astroglia within sections of rats treated with Kv after either NaN_3 (F) or $AlCl_3$ (G) appear normal than in groups D and E. Although group F shows considerably high GFAP immunodeposition, astroglia expression within group G is similar to the control. Again, Kv treatment normalized astroglia morphology in the hippocampus of rats that received it simultaneously with either NaN_3 (H) or $AlCl_3$ (I). Glia distributions across neurons in both groups are not different from those seen in control rats. (Scale bars: 50 μm)

corresponding groups. Rats treated with either of NaN_3 (D) or $AlCl_3$ (E) shows increased expression of astrocytes across hippocampal sections, with astrocyte clusters particularly seen in group F. Also, both groups show general morphological irregularities, as the different hippocampal areas are hardly appreciable. Hippocampal astrocytes expression within sections of rats treated with Kv after either NaN_3 (F) or $AlCl_3$ (G) are lesser than in groups D and E. Although group F shows considerably high GFAP immunopositivity, astrocytes expression within group G is similar to the control. Again, Kv shows strong inhibitory roles against astrogliosis as it normalized astrocytes deposition in the hippocampus of rats that received it simultaneously with either NaN_3 (H) or $AlCl_3$ (I). Glia expression, morphology and hippocampal distribution in both groups are not different from those seen in control rats.

Regarding neurofilaments microanatomy in this study, immunohistochemical staining of PFC sections (Fig. 9a) in the control rats, which were treated PBS (A), CO (B) or Kv (C), have normal expression of light chain neurofilaments. The cytoskeletal proteins have normal strand-like structural orientation, with even NF-l distribution observed in PFC sections within the three groups. However, NaN_3 (D) and $AlCl_3$ (E) treatment caused accumulation of NF-l subunits within the PFC of rats in this study. Also, very few neurofilament clusters can be seen in the PFC of rats treated with NaN_3 before kolaviron therapy (F), while rats that received $AlCl_3$ then Kv (H) showed normal NF-l prefrontal expression. In tandem with earlier findings, levels and patterns of NF-l expression within PFC of rats treated Kv simultaneously with either NaN_3 (H) or $AlCl_3$ (I) are not different from those expressed in rats that served as controls. Again, Fig. 9b shows immunohistochemical demonstration of NF-l within hippocampal sections of treated rats in this study. Control rats that were treated with PBS (A), CO (B) and Kv (C) have sparse neurofilament subunits with regular distribution across the well demarcated hippocampal morphology, which showed different cellular aspects clearly. In contrast, rats treated with either of NaN_3 (D) or $AlCl_3$ (E) showed enormous increase in hippocampal NF-l deposition. Hyperphosphorilation and aggregation of NF-l subunits in both groups are seen as clusters, across the poorly demarcated hippocampal regions. Similar to NF-l immunoexpression within PFC sections, very few dysregulated NF-l can be seen within hippocampal morphology of rats administered Kv after treatment with either NaN_3 (F) or $AlCl_3$ (G), showing the partial inhibitory role of Kv post-neurotoxicity. Again, rats treated simultaneously with Kv and either of NaN_3 (H) of $AlCl_3$ (I) have normal levels and patterns of NF-l expression/distribution within hippocampal sections of rats, same as in control groups. These findings underpin the neuroprotective roles of Kv against cytoskeletal dysregulation.

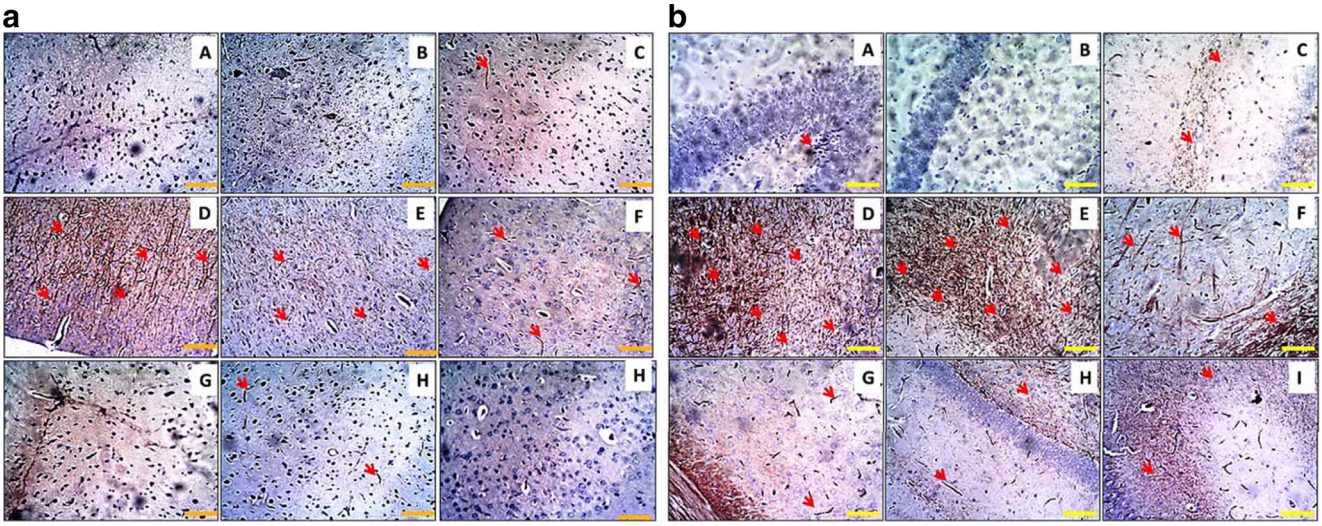

Fig. 9 **a** Immunohistochemical labelling of light chain neurofilaments (NF-l) in PFC sections of treated rats. Rats treated PBS (A), CO (B) and Kv (C) expressed NF-l with normal strand-like structural orientations which are evenly distributed across the neuropil. However, NaN_3 (D) and $AlCl_3$ (E) treatment induced dysregulation and accumulation of NF-l subunits within the PFC of rats (*red arrows*). Also, very few neurofilament clusters can be seen in the PFC of rats treated with NaN_3 before kolaviron therapy (F), while rats that received $AlCl_3$ then Kv (G) shows normal NF-l cortical expression. Furthermore, levels and patterns of NF-l expression within PFC of rats treated Kv simultaneously with either NaN_3 (H) or $AlCl_3$ (I) are normally expressed and not different from those expressed in rats that served as controls. (Scale bars: 50 μm). **b** Immunohistochemical labelling of NF-l in hippocampal sections of treated rats. Control rats that received PBS (A), CO (B) and Kv (C) have sparse neurofilaments subunits with regular distribution across the well demarcated hippocampal areas, which showed different cellular aspects clearly. In contrast, rats treated with either of NaN_3 (D) or $AlCl_3$ (E) showed marked increase NF-l deposition (*red arrows*). Hyperphosphorilated and aggregated NF-l subunits in both groups are expressed in clusters around degenerating neurons, and across poorly demarcated hippocampal regions. Very few dysregulated NF-l can be seen in hippocampal sections of rats administered Kv after treatment with either NaN_3 (F) or $AlCl_3$ (G). In addition, rats treated simultaneously with Kv and either NaN_3 (H) or $AlCl_3$ (I) shows normal levels and patterns of NF-l expression/distribution within hippocampal sections and is similar to control. (Scale bars: 50 μm)

Discussion

There are clear evidences to suggest that oxidative stress plays a crucial role in eliciting neurodegenerative disorders including Alzheimer's disease (Su et al. 2010; Swerdlow 2007). The hippocampal and PFC regions of AD brain appear to be particularly vulnerable to free radicals due to their low glutathione content, high proportion of polyunsaturated fatty acids and high demand for substantial quantity of oxygen for their proper metabolic activities. As oxidative damage is mediated by free radicals, it was necessary to investigate the status of endogenous antioxidant enzymes like SOD and GPx, which are the first line of defense against free radical damage under oxidative stress conditions. It was shown in the present study that $AlCl_3$ and NaN_3 depleted hippocampal and cortical level of SOD in rats as compared to control groups. As previously documented, depletion in neural levels of antioxidant enzymes greatly increase the susceptibility of the brain to amyloid β-peptide (Aβ)-induced toxicity, thereby leading to AD (Pocernich et al. 2011). Szabados et al. (2004) noted that NaN_3 exerts its neurotoxic effects through mitochondrial poisoning, while De Felice et al. (2007) showed that in hippocampal neurons, Aβ induces the formation of mitochondrial ROS by activating NMDA receptors. Aβ is further shown to enter the mitochondria and cause a signaling amplification that inactivates SOD and generates free radicals (Anantharaman et al. 2006). Therefore, it is suggestive that observed depletion of cortico-hippocampal SOD levels in this study is through increased generation of ROS, instigated by Aβ toxicity and mitochondrial damage.

Kv treatment improved SOD profiles within PFC and hippocampal lysates, particularly in rats that received it simultaneously with the neurotoxic compounds ($AlCl_3$ and NaN_3). Since SOD acts on O^{2-} to produce hydrogen peroxide (H_2O_2)-a relatively more stable ROS with lower oxidizing power (Sun and Trumpower 2003), its increment in neural cells by Kv may readily neutralize the cytotoxic effects of O^{2-} molecule. Another mechanism that may support positive maintenance of antioxidant profiles within cortico-hippocampal neurons by Kv may be through mopping up of the excessive free radicals produced from dysfunctional mitochondria, since the degree of oxidative damage is dependent on the balance between the oxidative stress and the efficiency of endogenous antioxidant mechanism that is found in the majority of cells.

Arguably the most prevalent antioxidant in the brain, glutathione (GSH) is capable of detoxifying ROS and neucleophilic compounds that are capable of initiating lipid peroxidation, which leads to neuronal membrane damage (Pocernich and Butterfield 2012). Treatment of rats with either of $AlCl_3$ and NaN_3 depleted the levels of GPx enzyme within both cortical and hippocampal cell lysates, as shown in obtained data. In AD, a decrease in the levels of GSH and its related enzymes, which is related to consistent increase in oxidative stress has been noted (Liu and Choi 2000). Taken in line with our current findings, this further shows that a mechanism involved in the toxicity of $AlCl_3$ and NaN_3 within PFC and hippocampus involves depreciation of GSH functions and enzymes. Furthermore, astrocytes have been shown as a major source of glutathione for neurons, while Al is documented to cause astrocytes apoptosis, therefore dramatically lowering neuronal glutathione levels (Murakami and Yoshino 2004). Another inhibitory mechanism of Kv shown by results from this study is in modulation of dysfunctional GSH antioxidant system, through normoregulation of GPx activities within cortico-hippocampal cells. It has been documented that a way of boosting defenses in the brain is by assisting the antioxidant defense system, particularly endogenous glutathione (GSH) and glutathione-related enzymes (Pocernich and Butterfield 2012). Similar to our observations, Ishola et al. 2016 showed that Kv inhibit scopolamine-induced oxidative stress by boosting GSH levels and inhibiting nitrating stress. Therefore, the inhibitory activity of Kv against imbalances of antioxidant enzymes may relate directly to prevention of propagation of the processes of lipid peroxidation and modulation of other cell death pathways in AD.

Various neurodegenerative pathologies are the consequence, and sometimes also the cause, of disturbed central or peripheral glucose bioenergetics, which can be affected at almost every levels of cellular or biochemical metabolic cascades. LDH and G6PDH are enzymes in the energy producing glycolytic pathway which may be affected by oxidative modification and decreased activity, and may contribute to the alteration in glucose metabolism noted in AD (Chen and Zhong 2013). LDH is released in vast quantity from neurons due to loss of membrane integrity, especially those caused by oxidative injury. Its aberrant production in cells is a useful tool for determining cytotoxicity and in measuring early cellular damage or impairment (Zhang et al. 2008). Rats treated with either of $AlCl_3$ or NaN_3 showed significant overexpression of LDH activities compared to the control groups in this study. Similarly, Jayasena et al. (2015) noted that impairment of mitochondria functions, exacerbated ROS production and neuronal bioenergetics alteration are implicated as early events in the pathogenesis of AD. Interestingly, rats that received Kv simultaneously with either of $AlCl_3$ or NaN_3 showed normal levels of LDH expression in both hippocampal and prefrontal lysates, unlike rats that received Kv after induced neurotoxicity-which showed partially improved cortical LDH expressions. A study found that the acetylation of LDH at K5 leads to degradation of LDH, through interaction with HSC70 chaperone and lysosomes (Zheng et al. 2004). Strong antioxidant agents like Kv are discussed to exert protective roles in cells through acetylation of toxic chemicals (Carocho and Ferreira 2013).

Unlike LDH expression in prefrontal and hippocampal lysates of treated rats, expression of G6PDH across treatment

groups was in no specific pattern in this study. There were no statistical significance in G6PDH activities within the separate hippocampal cells, while prefrontal levels of the enzyme is best described as erratically expressed between groups. G6PDH is the rate limiting enzyme of the pentose phosphate pathway (PPP), which is a glucose metabolizing pathway that determines the production of nicotinamide adenine dinucleotide phosphate (NADPH) by controlling glucose metabolism in the PPP. The produced NADPH is a critical modulator of redox potentials as it maintains the level of glutathione in cells that helps protect against oxidative damage (Nguyen et al. 2014). Our findings revealed that the expressed G6PDH in prefrontal cortex and hippocampus of rats treated with NaN_3 or $AlCl_3$ are not significantly different from other treatment groups. This result is quite intriguing and not in line with earlier findings of our study, and other reported studies, as it is widely known that depleted neural levels of G6PDH is a pathogenic similarity of many neurodegenerative disorders including AD (Jovanović et al. 2014; Olajide et al. 2015). Furthermore, with increased oxidative stress (such as demonstrated earlier), G6PDH expression and activity is seen to be upregulated in both in vivo and in vitro studies (Ansari and Scheff 2010; Russell et al. 1999; Yan 2014). Although statistically insignificant, it is noteworthy that rats which received Kv alone and after or simultaneously with $AlCl_3$ and NaN_3 expressed higher levels of G6PDH enzymes. This correlates with the findings of Olajide and Adeyemi (2011) that reported enhanced energy production in the intra-cranial visual pathway of rats via increased activity of G6PDH after treatment with extracts of *Garcinia kola*. Study by Adaramoye, (2012) also indicated the ability of Kv to regulate peripheral glucose levels in diabetic rats, indicating the its probable role in glucose bioenergetics control.

The prefrontal cortex and hippocampus show the earliest signs of neuronal death in AD, with this loss being the common pathway for a large number of degenerative processes in AD (Padurariu et al. 2012). Histopathological findings from this study showed that both NaN_3 and $AlCl_3$ initiated death of neurons within PFC and Hippocampus of rats. In those groups, neurons have characteristic hallmarks of apoptosis that applies to dying neurons, including shrinkage and condensation of soma and nuclear fragmentation, likely resulting from internucleosomal degradation of the DNA. Such cell death in chronic AD often occurs as a result of mutation in one or several genes (Armstrong 2009). The genetic alteration changes the function of gene product, in a way that has a detrimental effect on the cell and may account for neuronal loss seen in this study. A fact that supports cell death from genetic alterations in this study is the observed depletion of key antioxidant enzymes within PFC and hippocampus. Reduction in the level of the mitochondria matrix enzyme SOD, may reflect its inability to quench the cytotoxic effects of O^2•- by converting it to H_2O_2 which diffuses from mitochondria into the cytosol and nucleus. Concomitantly, low levels of GPx enzyme within PFC and hippocampal tissues may reflect failure in the detoxification of H_2O_2 within neuronal cytosol. Therefore, excess H_2O_2 may have been converted to OH or hydroxyl-like intermediates, while O^2•- reacts with the diffusible gas nitric oxide, to form the potent nucleophile oxidant and nitrating agent peroxynitrite (ONOO-). In turn, ONOO- which is genotoxic directly to neurons-by causing single and double-strand breaks in DNA (Segura-Aguilar and Kostrzewa 2004), may have activated proteins involved in cell cycle regulation of cell death as seen within PFC and hippocampus in this study. Administration of Kv however, abated neuronal apoptosis within both hippocampal and prefrontal tissues, particularly when administered alongside the neurotoxic compounds. The improvement of antioxidant profiles within neurons by Kv may have prevented damage within mitochondria complexes, subsequently preserving ATP production and more importantly eradicate electron leakage, accumulation of toxic reactive oxygen species, and release of apoptotic-inducing factors, that ultimately halted cell degeneration and death within cerebral and hippocampal tissues in this study. Another notable protective role played by Kv in this study, is the inhibition of dysfunctional axonal and dendritic connections to neurons as seen in higher power demonstration of the neurotoxic groups. Such damage can disrupt axonal transport by a variety of mechanisms, including the dysfunction of kinesin and cytoplasmic dynein, microtubules, cargoes, and mitochondria (De Vos et al. 2008). Furthermore, in preventing abnormal neuronal bioenergetics as seen earlier, Kv may have halted the biochemical cascade that activates proteases which destroy molecules expedient for cell survival, and others that mediate a program of cell suicide in neuronal apoptosis.

Roles of astrocytes and neurofilaments in neurodegeneration are crucial given their association with post transcriptional regeneration and regulation of axonal functions. Dysregulation in functions and structure of either or both neuronal supporting proteins initiates and exacerbate neurodegenerative processes within neurons in AD (Rodríguez et al. 2009; Yuan et al. 2012). Hypertrophic modification of astrocytes, seen in the accumulation of GFAP is a major pathological feature characteristic observed in AD (Ben Haim et al. 2015). Similarly, GFAP-positive cells, displaying typical morphology of reactive hypertrophied astrocytes are significantly elevated in both PFC and hippocampus of NaN_3 and $AlCl_3$ treated rats in the present study. Suárez-Fernández et al. (1999) observed that chronic Al exposure in mixed cultures of astrocytes and neurons results in significant astroglial apoptosis and associated neuronal loss. Our findings that Kv improves antioxidant profiles and quench cytotoxic free radicals within both prefrontal and hippocampal cells, may explain its role in the prevention of astrocyte hypertrophy. Furthermore, it has been shown that impairment of glutamate transporters,

through reduced expression, which results in increased synaptic glutamate and excitotoxicity, upregulates GFAP consistently with pathological features in neurodegenerative disease (Maragakis and Rothstein 2006). Therefore, the ability of Kv to prevent dysfunctional energy metabolism, through normoregulation of cortico-hippocampal LDH levels, may further explain its inhibitory role in astrogliosis and subsequent prevention of neuronal death. However, the rapid onset of degenerative cascades in rats pretreated with NaN_3 (in particular) and $AlCl_3$ before Kv therapy may underlie the partial inhibitory roles Kv has in preventing cortico-hippocampal hypertrophic astrogliotic changes. Additionally, the reactive astrocytes we found in the neurotoxic groups may also be responsible for the metabolic and oxidative imbalance found in cortico-hippocampal cells. One of the documented primary contributions of astrocyte to inflammatory processes in neurodegenerative diseases is in the production of neurotoxic molecules (Lewerenz and Maher 2015). The toxic compounds may have in turn suppressed antioxidant molecules and initiate aberrant glucose bioenergetics within neurons. Furthermore, activated astrocytes can attract microglia to jointly produce cytokines, coagulation factors, proteases and ROS (Cameron and Landreth 2010). These cytotoxic compounds may trigger neuronal death directly and may explain the corresponding neuronal apoptosis seen in cortical and hippocampal sections of rats treated NaN_3 (D) and $AlCl_3$. On the other hand, this phenomenon may also explain the neuroprotective mechanisms conferred by Kv on prefrontal and hippocampal cells. We suggest that Kv potentials to inhibit activated proteases and inflammatory proteins that resulted in astrogliosis may have halted further activation of excitotoxic stimuli and neuronal death.

In furtherance, neurofilaments are basic neuronal components of neuronal cytoskeleteton and they function primarily to provide structural support for the axon and to regulate axonal diameter (Zhu et al. 2009). Aggregations of this neuronal cytoskeletal protein is a pathological hallmark of neurodegenerative diseases, but peculiarities ranging from nature, molecular causes of cell death, time course and relationship to cytoskeletal pathologies are evident in the different forms of these disorders (Rami 2009). Findings from this study showed that PFC and hippocampus of rats treated either of NaN_3 and $AlCl_3$ are characterized by aggregated and hyperphosphorylated neurofilaments within the PFC and hippocampus. Similar to findings of this study, abnormally distributed light polypeptide neurofilaments have been documented in cortical and hippocampal tissues from AD patients (Gordon 2011). Additionally, the damaged axonal projections seen in histological demonstration of neurons in rats treated NaN_3 and $AlCl_3$ in this study, correlates with abnormal cytoskeletal microstructure. Our findings further highlight the efficacy of chronic exposures of both chemicals in producing pathogenic mechanisms of ADs in animals, which is necessary towards introduction of novel therapies for the debilitating diseases. In this connection, Kv treatment was shown to significantly inhibit hyperphosphorylation of light chain neurofilament within cortico-hippocampal neurons, particularly in rats that received it simultaneously with cytotoxic compounds. An interplay of degenerative conditions including; oxidative stress, excitotoxic stimulus, variations in neuronal Ca^{+2} levels, withdrawal of trophic support and dysfunctional bioenergetics have been described as primary factors responsible for disorganization and accumulation of neurofilaments in neuropathologic conditions (Sayre et al. 2008; Wagner et al. 2003). Intervention and halting the initiation and formation of toxic reactions of oxidative stress and glucose bioenergetics dysfunction may explain the modulatory roles of Kv in preventing neurofilament abnormalities, and may be central to it therapeutic mechanism in this study. Furthermore, neurons surrounded by mutant astrocytes develop protein aggregates and axonal pathology, and are more susceptible to cell death in several neurodegenerative disease models, including AD (Perlson et al. 2010). It is thereby suggestive, that the inhibition of astrocytes hypertrophy and mal-modification underlies mechanisms of Kv in preventing neurofilaments degeneration and the subsequent axonal damage in this study.

Conclusion

In conclusion, our study shows that chronic treatment of NaN_3 and $AlCl_3$ altered oxidative, bioenergetics, astrocytic, neurofilament and neuronal functions detectable in the prefrontal cortex and hippocampus of rats. Evidently, mechanisms underlying the degenerative cascades relating to these neurotoxic compounds were initiated in response to compromised mitochondrial function. Our observations lend support to an emerging body of evidence that both compounds successfully recapitulate important etiopathogenic factors of AD. We further showed that Kv inhibits cortico-hippocampal degeneration through multiple mechanisms that primarily involved halting of physiochemical imbalances, which originated subcellular neurodegenerative events seen in AD. We posit that the striking underlying and molecular inhibitory mechanisms of Kv, supports the idea that the compound be considered in strategies of using natural products in neurodegenerative disease therapy and particularly in their prevention.

Acknowledgements We acknowledge the technical support of Dr. Oso Babatunde Joseph for his technical assistance in the course of our analysis. We sincerely thank Olajide Oluwatomiyosi for proofreading this manuscript.

Compliance with ethical standards

Conflict of interest Authors declare that there are no actual or potential conflicts of interest including any financial, personal or relationships with other people or organizations within three years of beginning this work that could inappropriately influence, or be perceived to influence the study.

Funding This research did not receive any specific grant from funding agencies in the public, commercial, or not-for-profit sectors.

References

Adaramoye OA (2012) Antidiabetic effect of kolaviron, a biflavonoid complex isolated from *Garcinia kola* seeds. Wistar Rats Afr Health Sc 12:498–506

Anantharaman M, Tangpong J, Keller JN, Murphy MP, Markesbery WR, Kiningham KK, St. Clair DK (2006) β-amyloid mediated nitration of manganese superoxide dismutase: implication for oxidative stress in a APPNLh/NLh X PS-1 P264L/P264L double knock-in mouse model of Alzheimer's disease. Am J Pathol 168:5–15. doi:10.2353/ajpath.2006.051223

Ansari MA, Scheff SW (2010) Oxidative stress in the progression of Alzheimer disease in the frontal cortex. J Neuropathol Exp Neurol 69:155–167

Armstrong RA (2009) The molecular biology of senile plaques and neurofibrillary tangles in Alzheimer' s disease Senile plaques. Folia Neuropathol 47:289–299

Barbas H (2009) Prefrontal cortex: structure and anatomy. In: Squire LR (ed.) Encyclopedia of Neuroscience, volume 7, Oxford: Academic Press. pp 909–918

Ben Haim L, Carrillo-de Sauvage M-A, Ceyzériat K, Escartin C (2015) Elusive roles for reactive astrocytes in neurodegenerative diseases. Front Cell Neurosci 9:278

Cameron B, Landreth GE (2010) Inflammation, microglia, and alzheimer's disease. Neurobiol Dis 37:503–509

Carocho M, Ferreira ICFR (2013) A review on antioxidants, prooxidants and related controversy: natural and synthetic compounds, screening and analysis methodologies and future perspectives. Food Chem Toxicol 51:15–25

Chen Z, Zhong C (2013) Decoding Alzheimer's disease from perturbed cerebral glucose metabolism: implications for diagnostic and therapeutic strategies. Prog Neurobiol 108:21–43

De Felice FG, Velasco PT, Lambert MP, Viola K, Fernandez SJ, Ferreira ST, Klein WL (2007) A?? oligomers induce neuronal oxidative stress through an N-methyl-D-aspartate receptor-dependent mechanism that is blocked by the Alzheimer drug memantine. J Biol Chem 282:11590–11601

De Vos KJ, Grierson AJ, Ackerley S, Miller CCJ (2008) Role of axonal transport in neurodegenerative diseases. Annu Rev Neurosci 31: 151–173

Farombi EO, Adedara IA, Ajayi BO, Ayepola OR, Egbeme EE (2013) Kolaviron, a natural antioxidant and anti-inflammatory phytochemical prevents dextran sulphate sodium-induced colitis in rats. Basic Clin Pharmacol Toxicol 113:49–55

Farombi EO, Owoeye O (2011) Antioxidative and chemopreventive properties of Vernonia amygdalina and Garcinia biflavonoid. Int J Environ Res Public Health 8:2533–2555

Farombi EO, Shrotriya S, Surh YJ (2009) Kolaviron inhibits dimethyl nitrosamine-induced liver injury by suppressing COX-2 and iNOS expression via NF-??B and AP-1. Life Sci 84:149–155

Fischer AH, Jacobson KA, Rose J, Zeller R (2005) Hematoxylin and Eosin (H & E) staining. CSH Protoc 2008(4):pdb.prot4986

Gordon JA (2011) Oscillations and hippocampal-prefrontal synchrony. Curr Opin Neurobiol 21:486–491

Ishola IO, Adamson FM, Adeyemi OO (2016) Ameliorative effect of kolaviron, a biflavonoid complex from *Garcinia kola* seeds against scopolamine-induced memory impairment in rats: role of antioxidant defense system. Metab Brain Dis 32(1):235–245

Jayasena T, Poljak A, Braidy N, Smythe G, Raftery M, Hill M, Brodaty H, Trollor J, Kochan N, Sachdev P (2015) Upregulation of glycolytic enzymes, mitochondrial dysfunction and increased cytotoxicity in glial cells treated with Alzheimer's disease plasma. PLoS One. doi:10.1371/journal.pone.0116092

Jellinger KA (2010) Basic mechanisms of neurodegeneration: a critical update. J Cell Mol Med 14:457–487

Jovanović MD, Jelenković A, Stevanović ID, Bokonjić D, Čolić M, Petronijević N, Stanimirović DB (2014) Protective effects of giucose-6-phosphate dehydrogenase on neurotoxicity of aluminium applied into the ca1 sector of rat hippocampus. Indian J Med Res 139:864–872

Lanni C, Racchi M, Memo M, Govoni S, Uberti D (2012) P53 at the crossroads between cancer and neurodegeneration. Free Radic Biol Med 52:1727–1733

Lewerenz J, Maher P (2015) Chronic glutamate toxicity in neurodegenerative diseases-What is the evidence? Front Neurosci. doi:10.3389/fnins.2015.00469

Liu R, Choi J (2000) Age-associated decline in gamma-glutamylcysteine synthetase gene expression in rats. Free Radic Biol Med 28:566–574

Maragakis NJ, Rothstein JD (2006) Mechanisms of disease: astrocytes in neurodegenerative disease. Nat Clin Pr Neurol 2:679–689

Merelli A, Czornyj L, Lazarowski A (2013) Erythropoietin: a neuroprotective agent in cerebral hypoxia, neurodegeneration, and epilepsy. Curr Pharm Des 19:6791–6801

Murakami K, Yoshino M (2004) Aluminum decreases the glutathione regeneration by the inhibition of NADP-isocitrate dehydrogenase in mitochondria. J Cell Biochem 93:1267–1271

Nguyen TTM, Kitajima S, Izawa S (2014) Importance of glucose-6-phosphate dehydrogenase (G6PDH) for vanillin tolerance in *Saccharomyces cerevisiae*. J Biosci Bioeng 118:263–269

Olajide OJ, Adeyemi AP (2011) Studies on effects of aqueous Garcinia kola extract on the lateral geniculate body and rostral colliculus of adult. Wistar Rats 2:23–28

Olajide OJ, Enaibe BU, Bankole OO, Akinola B, Laoye BJ, Ogundele OM (2015) Kolaviron was protective against sodium azide (NaN 3) induced oxidative stress in the prefrontal cortex. Metab Brain Dis 31:25–35

Oyenihi OR, Brooks NL, Oguntibeju OO (2015) Effects of kolaviron on hepatic oxidative stress in streptozotocin induced diabetes. BMC Complement Altern Med 15:236

Padurariu M, Ciobica A, Mavroudis I, Fotiou D, Baloyannis S (2012) Hippocampal neuronal loss in the CA1 and CA3 areas of Alzheimer's disease patients. Psychiatr Danub 24:152–158

Patten DA, Germain M, Kelly MA, Slack RS (2010) Reactive oxygen species: stuck in the middle of neurodegeneration. J Alzheimer's Dis. doi:10.3233/JAD-2010-100498

Perlson E, Maday S, Fu M, Moughamian AJ, Holzbaur ELF (2010) Retrograde axonal transport: pathways to cell death? Trends Neurosci 33:335–344

Pocernich CB, Bader Lange ML, Sultana R, Butterfield DA (2011) Nutritional approaches to modulate oxidative stress in Alzheimer's disease. Curr Alzheimer Res 8:452–469

Pocernich CB, Butterfield DA (2012) Elevation of glutathione as a therapeutic strategy in Alzheimer disease. Biochim Biophys Acta - Mol Basis Dis 1822:625–630

Rami A (2009) Review: autophagy in neurodegeneration: firefighter and/or incendiarist? Neuropathol Appl Neurobiol 35:449–461

Reitz C, Brayne C, Mayeux R (2011) Epidemiology of Alzheimer disease. Nat Rev Neurol 7:137–152

Reitz C, Mayeux R (2014) Alzheimer disease: epidemiology, diagnostic criteria, risk factors and biomarkers. Biochem Pharmacol 88:640–651

Rodella LF, Ricci F, Borsani E, Stacchiotti A, Foglio E, Favero G, Rezzani R, Mariani C, Bianchi R (2008) Aluminium exposure induces Alzheimer's disease-like histopathological alterations in mouse brain. Histol Histopathol 23:433–439

Rodríguez J, Olabarria M, Chvatal A, Verkhratsky A (2009) Astroglia in dementia and Alzheimer's disease. Cell Death Differ 16:378–385

Russell RL, Siedlak SL, Raina AK, Bautista JM, Smith MA, Perry G (1999) Increased neuronal glucose-6-phosphate dehydrogenase and sulfhydryl levels indicate reductive compensation to oxidative stress in Alzheimer disease. Arch Biochem Biophys 370:236–239

Sayre LM, Perry G, Smith MA (2008) Oxidative stress and neurotoxicity. Chem Res Toxicol 21:172–188

Segura-Aguilar J, Kostrzewa RM (2004) Neurotoxins and neurotoxic species implicated in neurodegeneration. Neurotox Res 6:615–630

Serrano-Pozo A, Frosch MP, Masliah E, Hyman BT (2011) Neuropathological alterations in Alzheimer disease. Cold Spring Harb Perspect Med. doi:10.1101/cshperspect.a006189

Su B, Wang X, Lee H-G, Tabaton M, Perry G, Smith MA, Zhu X (2010) Chronic oxidative stress causes increased tau phosphorylation in M17 neuroblastoma cells. Neurosci Lett 468:267–271

Suárez-Fernández MB, Soldado AB, Sanz-Medel A, Vega JA, Novelli A, Fernández-Sánchez MT (1999) Aluminum-induced degeneration of astrocytes occurs via apoptosis and results in neuronal death. Brain Res 835:125–136

Sun J, Trumpower BL (2003) Superoxide anion generation by the cytochrome bc1 complex. Arch Biochem Biophys 419:198–206

Swerdlow RH (2007) Pathogenesis of Alzheimer's disease. Clin Interv Aging 2:347–359

Szabados T, Dul C, Majtényi K, Hargitai J, Pénzes Z, Urbanics R (2004) A chronic Alzheimer's model evoked by mitochondrial poison sodium azide for pharmacological investigations. Behav Brain Res 154:31–40

Trushina E, McMurray CT (2007) Oxidative stress and mitochondrial dysfunction in neurodegenerative diseases. Neuroscience 145: 1233–1248

Wagner OI, Lifshitz J, Janmey PA, Linden M, McIntosh TK, Leterrier J-F (2003) Mechanisms of mitochondria-neurofilament interactions. J Neurosci 23:9046–9058

Wood JPM, Mammone T, Chidlow G, Greenwell T, Casson RJ (2012) Mitochondrial inhibition in rat retinal cell cultures as a model of metabolic compromise: mechanisms of injury and neuroprotection. Investig Ophthalmol Vis Sci 53:4897–4909

Yan LJ (2014) Pathogenesis of chronic hyperglycemia: from reductive stress to oxidative stress. J Diabetes Res. doi:10.1155/2014/137919

Yuan A, Rao MV, Veeranna, Nixon RA (2012) Neurofilaments at a glance. J Cell Sci 125:3257–3263

Zhang X, Yang F, Xu C, Liu W, Wen S, Xu Y (2008) Cytotoxicity evaluation of three pairs of hexabromocyclododecane (HBCD) enantiomers on Hep G2 cell. Toxicol Vitr 22:1520–1527

Zheng Y, Guo S, Guo Z, Wang X (2004) Effects of N-terminal deletion mutation on rabbit muscle lactate dehydrogenase. Biochem 69:401–406

Zhu X, Liu Y, Yin Y, Shao A, Zhang B, Kim S, Zhou J (2009) MSC p43 required for axonal development in motor neurons. Proc Natl Acad Sci USA 106:15,944–15,949